Chemical Engineering Journal 481 (2024) 148278

Contents lists available at ScienceDirect

Chemical Engineering Journal

journal homepage: www.elsevier.com/locate/cej

Process development and techno-economic analysis for mechanochemical recycling of poly(ethylene terephthalate)

Elisavet Anglou [1], Arvind Ganesan [1], Yuchen Chang, Kinga M. Gołąbek, Qiang Fu, William Bradley, Christopher W. Jones, Carsten Sievers, Sankar Nair [*], Fani Boukouvala [*]

School of Chemical & Biomolecular Engineering, Georgia Institute of Technology, Atlanta, GA 30332, USA

ARTICLE INFO

Keywords:
Ball milling
Mechanochemical reactor
PET
Techno-economics
Monomers
Separations
Process flow modelling
Recycling

ABSTRACT

Chemical recycling of consumer plastics has garnered great attention recently towards achieving circular economy goals. Particularly in the case of PET waste, mechanochemical depolymerization in ball mill reactors has been identified as a very promising technology due to the high conversion rates achieved under mild conditions. While the absence of solvents in the reaction mixture reduces significant separation costs, mechanochemical depolymerization still presents challenges with respect to the efficient separation and purification of monomers. Thus, meticulous experiments, process modeling, and simulations are essential for demonstrating the separation and purification of monomers. In this study, we present the lab-scale separation process flow for the recovery of terephthalic acid (TPA) and ethylene glycol (EG) from mechanochemically depolymerized polyethylene terephthalate (PET). We additionally examine the use recycling of ideal PET powder and commercial samples (e.g., PET fibers, bottles, and food containers) as feedstocks. The process parameters are optimized to achieve 97 %+ of monomer recovery with 99 %+ purity. The complete recovery of EG, and recycling of process water enables a 'zero-liquid discharge' process design. Subsequently, we conduct a techno-economic analysis (TEA) to evaluate the economic potential of the proposed sequence, which resulted in a positive net present value (NPV) for the different scenarios and a minimum selling price (MSP) of $0.99/kg. Finally, we compare the economic potential of mechanochemical recycling of PET to fossil-based production and other recycling methodologies based on economic metrics.

1. Introduction

Plastics have revolutionized our daily lives due to their chemical stability, durability, and low cost, and have gradually replaced other materials such as glass, steel, or wood across a wide range of applications [1,2]. However, a significant amount of plastics ends up in landfills and marine environments [3–5]. As of 2018, the global production of plastic reached 359 million tons [6]. A mere 10 % of the total plastic volume collected is recycled, with just 2 % processed through closed-loop recycling [7], while the majority (79 %) is left to accumulate in landfills or other natural environments [1]. Geyer et al. [1] project the annual production of plastics to reach 1.1 billion tons by 2050. In addition to interference in natural habitats [8,9], the breakdown of plastics into microplastics [10] and toxic water-soluble chemicals [11] has garnered increasing attention in the context of their environmental and economic implications. Thus, the effective management of plastic waste and their end-of-life treatment stands as a major challenge. Specifically, there is a growing interest in transitioning to a circular economy (CE) in which plastics will be efficiently and sustainably recycled back into the economy.

Poly(ethylene terephthalate) (PET) amounted to over 32 million metric tons of global annual plastic production in 2019 [12]. PET is made by the co-polymerization of terephthalic acid (TPA) and ethylene glycol (EG) via esterification, and is widely used to make beverage bottles, packaging, carpets, and clothing. Currently, processing of PET waste through mechanical recycling is the most widely implemented technology [13–16]. However, mechanical recycling usually leads to degradation of the functional properties of PET waste due to the mechanical and thermal stresses/breakdown acting on the polymer during reprocessing [2,7,17]. Consequently, PET can be mechanically recycled only a limited number of times and only if mixed with large quantities of virgin polymers [18,19].

* Corresponding authors.
E-mail addresses: sankar.nair@chbe.gatech.edu (S. Nair), fani.boukouvala@chbe.gatech.edu (F. Boukouvala).
[1] Authors contributed equally.

https://doi.org/10.1016/j.cej.2023.148278
Received 6 September 2023; Received in revised form 6 December 2023; Accepted 20 December 2023
Available online 23 December 2023

Alternatively, the relative ease of cleaving an ester bond (C-O), as compared to C-C bonds in other polymers, has generated greater interest in the chemical recycling of PET into monomers [2,17]. Chemical recycling, although less common, has emerged as a promising alternative to traditional recycling methods. Polymers are directly converted to monomers or oligomers that may be further purified to the same molecules as virgin materials, thus avoiding degradation of physical and chemical properties, and stepping towards a circular plastics sector with lower dependence on petrochemical feedstock [2,20–23]. Solvent-assisted chemical breakdown of PET (solvolysis) has made large progress over the last decade [2,22]. Hydrolysis of PET in acidic [24–26], basic [27–30], and neutral [31,32] conditions are widely studied. Glycolysis [33–35] and (more generally) alcoholysis [36–38] are also explored for homogeneous depolymerization of PET. Typically, these conventional processes operate at high temperatures (100–300 °C) and pressures (up to 20 bar) with high solvent-to-PET ratios (from 5 to 20), driving up the depolymerization and separation costs.

In contrast, the advent of mechanochemical depolymerization creates a potential paradigm change [19,39,40]. The depolymerization reaction is performed in a ball mill, and the energy necessary to drive the reaction is supplied to the system through the impacts of the balls with solid particles [2]. This approach has distinct advantages: (a) it does not require a reaction solvent nor extreme operating conditions, and (b) the ball mill uses electrical energy input rather than process heating. Mechanochemical routes has been recently demonstrated for the depolymerization of various types of plastics including PET, PS, PVC and others [41–47]. The conversion of plastics into value-added products are exciting alternatives [45,46]. Specifically for the case of PET, Strukil et al. [39] recently reported a high conversion of PET to monomers via milling. Tricker et al. [19] demonstrated complete depolymerization of PET and stoichiometric amounts of sodium hydroxide (NaOH) to ethylene glycol (EG) and disodium terephthalate salt (Na_2TPA).

Mechanochemical PET depolymerization presents new opportunities and challenges in the development of overall processes that are economically viable. For example, the solid depolymerization products from the ball mill consist of monomers, unreacted polymers (if any), catalysts (if any), and other impurities (dyes, additives, etc.) originating from the feedstock. These pose new separation issues compared to conventional solvolysis, which generally results in a multicomponent mixture that is also prone to the formation of azeotropes. Thus far, solvolysis processes have used separation processes such as filtration (to remove unreacted polymers) and crystallization of TPA or BHET by acidification or drying [29,33,37,48]. Recently, Singh et al. [49] also addressed the large cost of separating EG from excess solvent in conventional solvolysis.

Process simulators such as Aspen Plus [50] or gProms [51] are used to obtain the mass and energy flows, which then allows for the quantitative comparison of different scenarios or sequences of unit operations [52–55]. By coupling these simulation results with costing correlations or other information from manufacturers, the fixed and operating expenses can be determined. This enables the comprehensive assessment of how the design variable impact the projected economics [56,57]. While there is a significant body of literature on PET depolymerization, only limited information is available on the techno-economic aspects of PET chemical recycling technologies [49,56,58]. Particularly for the case of PET plastic waste, Singh et al. [49] performed a technoeconomic analysis (TEA) and life cycle assessment (LCA) to evaluate the social and economic implications of an enzyme-catalyzed depolymerization process for PET. Their analysis suggested that enzymatic depolymerization recycling could be economically feasible relative to the production of new (petro-derived) PET. The projected minimum selling price (MSP) for this method ($1.93/kg) was found to be higher than the market averages (currently $1.14/kg for virgin TPA), but the sensitivity analysis revealed that the MSP could drop if higher conversion rates could be achieved. Uekert et al. [57] conducted a comparative evaluation of the previously known recycling routes for PET (and other plastics) using various economic and sustainability metrics. Their findings indicate that glycolysis offers the best overall performance for PET recycling, with an MSP of $0.96/kg (BHET) that is competitive with the prices of virgin PET. To the best of our knowledge, quantitative process and economics analysis have not been performed yet for mechanochemical or mechanocatalytic depolymerization pathways.

In this work, we combine lab-scale experimental design, validation, and a process systems engineering approach to design, simulate, and optimize an integrated process flowsheet that facilitates the mechanochemical depolymerization of PET waste to its monomeric molecules (Fig. 1). The primary products of the mechanochemical reaction of PET with sodium hydroxide (NaOH) are disodium terephthalate (Na_2TPA) and ethylene glycol (EG). A sequence of unit operations is designed and validated experimentally to facilitate the selective extraction, purification of individual monomers. The depolymerization of ideal (PET powder) and commercial feedstocks (textiles, PET bottles and food containers) are studied. Subsequently, the process flowsheet is modeled in the Aspen Plus using pre-defined and custom-defined unit operation models. The flowsheet is designed for a scaled-up process, with throughput rates estimated based on total PET recycling rates in the state of Georgia, USA. Calculations of mass and energy flow are utilized to determine equipment sizing and utility requirements. A techno-economic analysis (TEA) is then conducted. These integration of all these tools and results enable the assessment of the future economic potential of the process. Through sensitivity analyses, the significance of process design variables such as reactor or separations specifications, as well as the impact of feedstock and raw material price volatility on the projected minimum selling price (MSP) is quantified.

The rest of the paper is organized as follows. Section 2 highlights the methods used in the experimental and computational part of the work. Section 3 provides an overview of the proposed flowsheet design and discusses the experimental validation, explores the techno-economics of the integrated process and presents the results of the sensitivity analyses. Finally, Section 4 summarizes the conclusions of the work and outlines future prospects.

2. Experimental and modeling methods

2.1. Materials

Poly (ethylene terephthalate) (PET) granules (semi-crystalline >50 %, Sigma Aldrich), commercial Kolon textiles (brown color), clear PET bottles and food containers, sulfuric acid (VWR), disodium terephthalate (Alfa Aesar), acetone (VWR), sodium sulfate (Sigma Aldrich), D_2O (Sigma Aldrich), Sodium trimethylsilylpropanesulfonate (Fischer Scientific), deuterated trifluoroacetic acid (TFA-d) (Sigma Aldrich), and sodium hydroxide (Sigma Aldrich). Deionized water from the EMD Millipore water purification system, DuPont FilmTec XC70, Whatman filter papers, and VWR 0.2 μm syringe filter were used in this work.

2.2. Composition analyses

Solution NMR measurements were performed with Bruker Avance III 400 MHz. SEM images were obtained with Hitachi SU 8010 scanning electron microscope. Solvent recovery was performed with Buchi Rotavapor R-100. SO_4^{2-} ions are measured by IC. The ion chromatography measurements were performed with a Shimadzu HPLC system equipped with a conductivity detector (Shimadadzu, CDD-10AVP, USA). IonPac® AS11 (250 mm × 2 mm ID) was used with a column temperature of 30 ℃, mobile phase of 10 mM NaOH (0.30 mL/min) and injection volume is 1 μL. SEM images of the TPA crystals were obtained with Hitachi SU 8230 scanning electron microscope.

2.3. Extraction of EG and Na_2TPA

Typically, the depolymerized mixture was dispersed in acetone (1:1

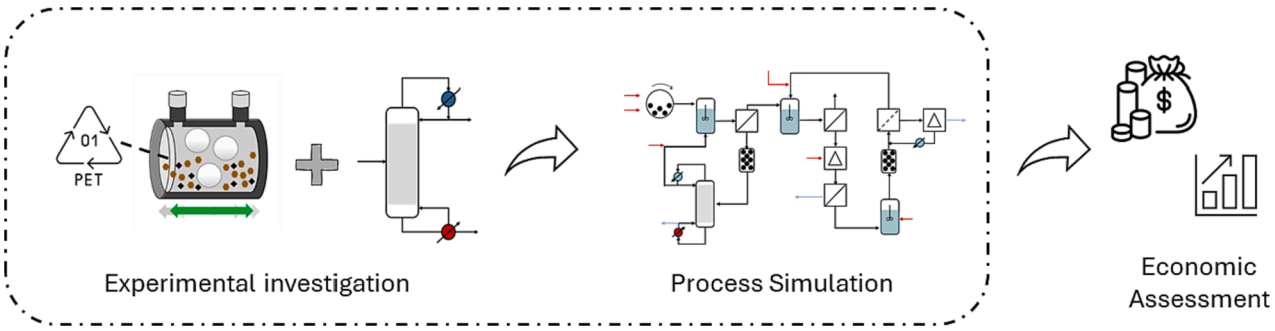

Fig. 1. Workflow of the present analysis.

mass ratio), the mixture was stirred at 200 rpm for 5 min, and subsequently filtered with a 0.2 μm syringe filter. The recovery of EG from the acetone stream was performed with a rotary evaporator at 370 mbar, 50 °C. Na_2TPA was extracted by washing with water (maintain Na_2TPA under 10 wt%). Unreacted PET (if any) was separated with a 0.2 μm PTFE filter. TPA was crystallized and precipitated by slow addition of conc. H_2SO_4 (0.5 mL/min) to the aqueous solution of Na_2TPA. TPA crystals were isolated with a 5 μm polycarbonate filter. The crystals were dried at 50 °C overnight. EG and TPA recoveries were estimated with solution NMR measurements with D_2O as the solvent.

2.4. Water recovery

Salt rejection (Na_2SO_4) measurements on a DuPont FilmTec XC70 were performed in a Sterilitech high-pressure dead-end stirred cell (HP4750X) with 300 mL volume feed capacity. Ion rejection performances were evaluated with Ion Chromatography (IC).

2.5. Process simulations

2.5.1. Ball Mill Reactor Simulation

The industrial ball milling configuration typically involves a rotating cylindrical vessel filled with grinding balls and reactants (e.g, PET waste and NaOH particles). High-fidelity Discrete Element Method (DEM) simulations were performed in the EDEM commercial software [59] based on the operating parameters listed in Table 1 to determine the required torque requirements to rotate the mill. Fig. 2 shows a visual representation of the simulation setup. The Hertz-Mindlin (no-slip) contact model was selected as it is appropriate for spherical shapes and has been previously utilized in similar ball-milling applications. The material and contact parameters that are required as inputs to DEM simulations were taken from the available milling literature [60]. A rotating cylindrical geometry is designed for the industrial ball-mill reactor. Based on the experimental findings of our previous study, the achieved monomer yield follows a linear relationship with the ball-to-powder mass ratio (BPR) parameter [19]. If the industrial-scale ball mill reactor can maintain equivalent BPR values, the number of grinding balls and the size of the reactor can be evaluated for a constant PET waste feed. Higher BPR values correspond to higher yields with full depolymerization achieved when BPR = 22.9 with a reaction time of 20 min. In the context of this work, a BPR of 22.9 was used to design the reactor and the operating conditions. Results from the DEM simulations are used for the evaluation of the annual electricity cost for the ball milling system. The maximum torque load requirements were extracted from the high-fidelity DEM simulation. Based on the selected operating settings, the energy consumption of the ball-mill reactor was estimated at 122 kW. The required capital expenditure is calculated using the correlations provided by Seider [61]. Our previous work provides a more detailed analysis on the selection of operating conditions that lead to 100 % conversion, the evaluation of the capital expenditure of the ball-mill reactor and the estimation of the energy consumption [62].

Table 1
Operating settings of the ball mill reactor.

Parameter	Value
Volume (m^3)	45
Number of balls	9016
r_{ball} (mm)	60
Fill-level (%)	30
Conversion	100
Ball-to-Powder ratio	22.9

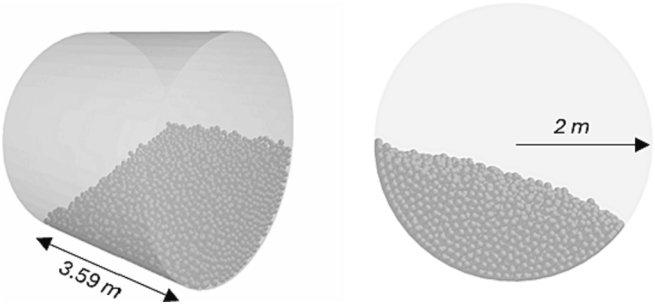

Fig. 2. The industrial ball mill reactor as designed and simulated in the EDEM software.

The ball mill consumables include media consumption (stainless-steel balls) and play a crucial role in the grinding process. Over time, due to the wear and tear, the balls need to be replaced on a regular basis determined by the wear rate of the ball charge [63,64]. In the cement industry, the replacement period is scheduled based on a wear rate of 35 – 70 $gram_{steel}$/metric ton whereas for limestone grinding a wear rate of 500 $gram_{steel}$/metric ton is typically used [63,64]. In the context of our application, a wear rate of 50 $gram_{steel}$/metric was selected as a more conservative scenario, given that the PET polymers are expected to be less hard than cement or limestone. The total steel mass is evaluated, and the replacement cost is estimated based on the all-in steel rate (US $4300/metric ton) [64].

2.5.2. ASPEN flowsheet simulation of integrated process

After the integrated process (reactors, separators) was designed and demonstrated experimentally at the lab-scale, the flowsheet was modeled in Aspen Plus V12 (Aspen Technology Inc.) [50]. A processing capacity of 48 metric tons per day of PET waste was simulated, equivalent to an hourly input rate of 2,000 kg/hr. This is based on the amount of PET waste recycled in the state of Georgia, USA for 2018 as reported by the National Association for Plastic Container Resources (NAPCOR) [65]. Most of the reaction components were chosen from the existing Aspen databases while those that were not available were defined based on their molecular structures and boiling points. Other physical properties were retrieved from the NIST database or estimated via Aspen Plus Properties Constant Estimation System (PCES).

The mass balances for all the purification steps were validated through experiments as described in the previous subsection. Throughout this work, it is assumed that the laboratory-scale conversions and separation efficiencies can be maintained at a larger scale. All the design parameters entered in the Aspen Plus simulation are summarized in Table 2. These parameters were experimentally validated at the laboratory scale (see Results and Discussion).

2.6. Economic analysis

Operating (e.g., raw material, utility costs) and capital (equipment sizing) expenditures were estimated based on the material and energy balance results from the Aspen simulation while additional costs such as labor and maintenance expenses are calculated based on chemical engineering heuristics [61]. The purchasing costs were estimated through the well-established correlations and scaling factors reported in Seider [61], taking into consideration the required size and type of materials for each piece of equipment as well as the corresponding installation factor. All the costs were extrapolated to the 2022-dollar value using the Chemical Engineering Process Cost Index (CEPCI).

$$\text{Current Cost} = (\text{Cost in year i})\frac{\text{Current Index}}{\text{Index in year i}} \quad (1)$$

Based on these assumptions, the total capital investment (TCI) is calculated. TCI includes the direct (equipment, installation, piping, etc.) and indirect costs (engineering, contractor fees, etc.) associated with the construction of a manufacturing facility. TCI also incorporates the working capital, which is the amount that should be available to finance the early operation of the plant.

Additionally, to complete the techno-economic analysis for the plant, estimations for the annual operating costs and sales profit are required. The cost of production is calculated as the sum of the cost of manufacture and general expenses which typically includes direct manufacturing costs (such as feedstocks, utilities, etc.), operating overhead, fixed costs (property taxes, depreciation, etc.), and general expenses (related with the central operation of the company). Prices of raw materials, products, and by-products are obtained from a recent study by Singh et al. [49] that provides a comprehensive analysis of the price trends over the previous decade. The average of prices reported between 2012 and 2016 are utilized in the context of this analysis. A detailed breakdown of all the prices used can be found in the SI (Table S9 and Table S10). The cost of pretreatment including shredding and cleaning of the postconsumer plastic bales is integrated in the price of PET flakes ($0.55/kg). The complete set of prices is summarized in Table 3.

Table 2
Summary of the parameters and design specifications in the baseline model setup.

Unit	Block	Design variable	Baseline case
Ball mill	DEM simulation	Conversion	100 %
Distillation column	RadFrac	Number of trays	6
		Reflux ratio	1.2
Acidification reactor	RStoic	Equilibrium reaction	
Neutralization reactor	RStoic	Equilibrium reaction	
Pump	Pump	Isentropic efficiency	0.8
Filter 1	Separator	Solid separation efficiency (slurry)	1
Filter 2	Separator	Solid separation efficiency (PET)	1
Filter 3	Separator	Solid separation efficiency (TPA)	0.98
Crystallizer	Crystallizer	Temperature (°C)	14.4
		Pressure (bar)	1

Table 3
Raw material, product, and utility prices.

	Cost ($/kg)	Reference
Products		
TPA	1.14	[49]
Ethylene Glycol	0.96	[49]
Na_2SO_4	0.15	[49]
Raw Materials		
PET	0.55	[49]
Acetone	0.91	[66]
NaOH	0.61	[49]
H_2SO_4	0.10	[49]
Utilities		
Process water	$ 0.27/m^3	[61]
Cooling water	$ 5/GJ	[61]
Electricity	$ 0.07/kW-h	[61]
Refrigerant	$ 6.47/GJ	[61]

The Net Present Value (NPV) is an indicator often used to assess the profit potential of industrial processes[53,67]. The NPV represents the surplus generated by an investment at the beginning of the planning horizon relative to the return rate applied and provides insights into the time value of money by discounting future cash flow to their present worth. To evaluate NPV, a discounted cash flow analysis was conducted (Eq. (2)).

$$\text{NPV} = -Z_0 + \sum_{t=0}^{T}\frac{\text{Annual CF}_t}{(1+\text{RR})^t} \quad (2)$$

Here, Z_0 represents the initial investment in $, RR the rate of return, while CF_t denotes the annual cashflow at time t.

In addition, we utilized the minimum selling price (MSP) as an economic indicator to facilitate comparisons between the proposed technology, competing processes, and present market prices. The MSP corresponds to the price that generates an NPV value equal to zero [67,68]. In other words, a break-even assessment was performed to identify the selling price of the main product (TPA) after which the process becomes profitable.

The depreciation method employed for this project is a 10-year MACRS, with a two-year startup time, with no profit during the first two years. The facility is assumed to operate at three 8 h/day shifts for 330 days/year. A return rate of 10 % is utilized to evaluate the present value of future cash flows, while the inflation rate was set at 2 %. All the financial parameters employed in this work are depicted in Table 4.

3. Results and discussion

3.1. Overview of the process flow diagram

Fig. 3 illustrates the simplified process flow diagram for the mechanochemical hydrolysis of PET waste, including the depolymerization reactor unit and all the subsequent product recovery steps. The designed facility processes 2000 kg/h (~15,840 MT/year) of PET and generates

Table 4
Economic assumptions.

Parameter	Value
Feedstock rate	2000 kg/h
Annual interest rate	10 %
MACRS depreciation	10 years
Taxation rate	26 %
Inflation rate	2 %
Project life	12 years
Construction period	2 years
Working capital	10% of Raw Materials Cost

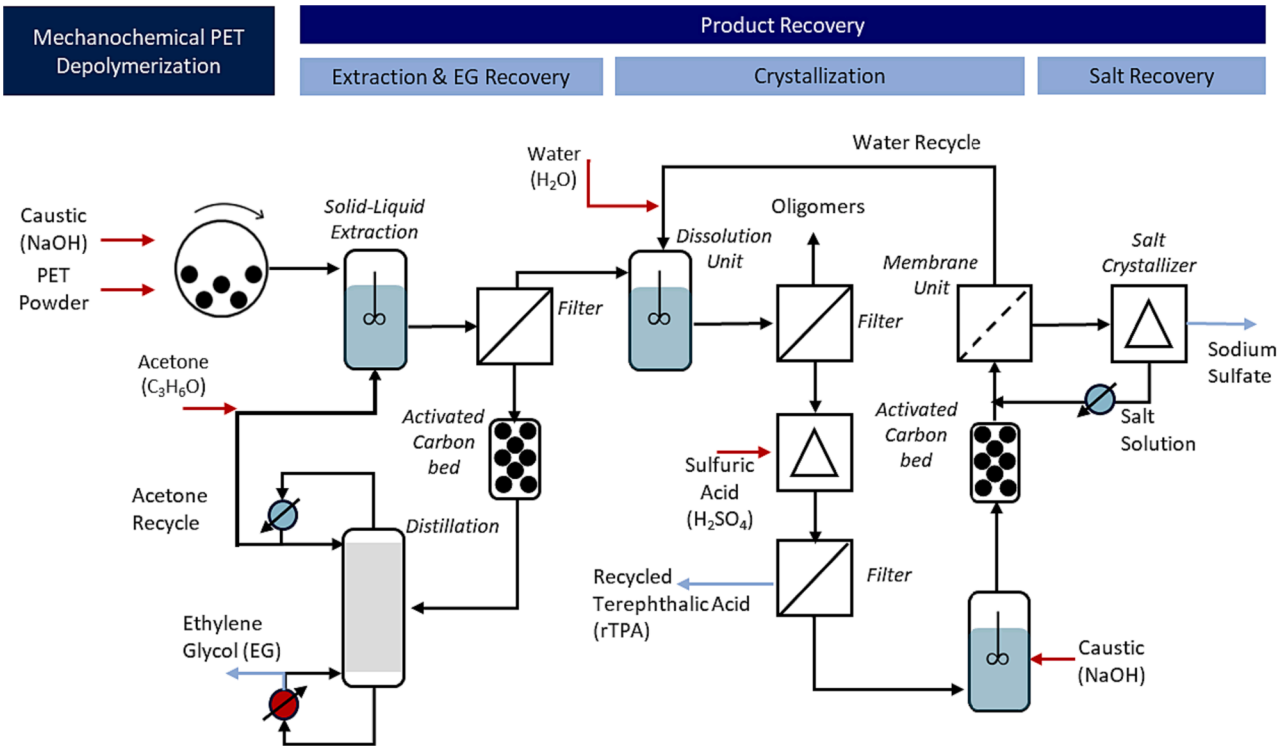

Fig. 3. Baseline case process for mechanochemical depolymerization of PET waste, divided into depolymerization and product recovery sections. Input streams are illustrated in red while product streams are in blue. (For interpretation of the references to color in this figure legend, the reader is referred to the web version of this article.)

approximately 1935 kg/h (~15,325 MT/year) of terephthalic acid (TPA) and 737 kg/h (~5,837 MT/year) of ethylene glycol (EG), which can be utilized directly in the production of new PET products.

Clean PET powder flakes are obtained from a pre-treatment facility under the assumption that the whole feed is recyclable, and the concentration of impurities is negligible. As reported by Tricker et al. [19], high depolymerization yields ranging from 80 to 100 % were achieved in the ball mill reactor at the laboratory scale when using PET waste feedstock in the form of powder with particle sizes in the range of 0.3 mm for the operating setting that promote complete conversion as discussed in *Section 2.5*. The baseline analysis assumes the use of clean and uncontaminated PET flakes, providing a conservative estimate for the recycled terephthalic acid (rTPA) price. Depolymerization experiments were also conducted using commercial PET bottles and food containers as inputs to illustrate the robustness of the process. Further discussion on the use of non-ideal feedstocks is provided in Sections 3.2 and 3.4. Prior to the depolymerization section, several feedstock pretreatment steps were also introduced to account for the cost required to transfer the PET flakes from storage to the reactor (conveyor belt, storage space and tanks, truck dumper). The pre-treatment steps were only accounted for in economics and were not simulated in Aspen Plus.

The plastic waste powder is introduced into the ball mill reactor along with the NaOH particles and is converted into the monomers disodium terephthalate (Na_2TPA) and ethylene glycol (EG). Following the mechanochemical depolymerization reaction, the ball mill reactor outlet stream (e.g, Na_2TPA + EG) is processed through a solid-liquid extraction and a filtration unit. Acetone is used to selectively extract EG from Na_2TPA, and the resulting slurry is passed through a filter to separate the solids (Na_2TPA, additives, and any unreacted PET). An activated carbon column is installed to remove any dyes, pigments, or adhesives present in the acetone + EG stream. EG and acetone are then separated in a distillation column with a purity over 99 % and 99 %+ recovery.

The Na_2TPA from the solids (Na_2TPA and unreacted PET), is selectively dissolved in water (H_2O) at a mass ratio of 1:9 and filtered to separate any residual PET. In the scenario that full depolymerization is not achieved, residual PET can be recycled back to the ball mill. Sulfuric acid (H_2SO_4) is then added slowly to the resulting aqueous solution of Na_2TPA to precipitate rTPA (recycled terephthalic acid) in a continuous crystallizer. The resulting rTPA crystals are then retrieved at a purity of 99 %. The precipitation and filtration step recovers 97 %+ of the monomer, as observed experimentally. An activated column is installed to separate any traces of rTPA that were not collected from the aqueous solution.

The aqueous solution exiting the activated carbon column, is neutralized with caustic (NaOH) and processed in a reverse osmosis membrane unit with 63.6 % water recovered. The permeate (process water) is returned to the dissolution unit, while the retentate is routed to a cooling crystallization unit for the recovery of sodium sulfate (SS). The SS crystals (also known as Glauber's salt) are produced and are collected as a byproduct. The saturated solution is recycled to the membrane to recover water and concentrate the SS aqueous solution (rerouted back to the salt recovery section). Table 5 presents the feedstock, resulting product, and co-products mass flow rates, while Table 6 summarizes the reactions involved throughout the integrated process. A figure depicting the Aspen Plus simulation is provided in the SI (Fig. S5).

3.2. Experimental results

Fig. 4 shows the solution NMR data of the depolymerized mixture,

Table 5
Feed, product, and by-products quantities.

	Unit	Baseline case
PET waste (feed)	kg/h	2000
rTPA (product)	kg/h	1935
Ethylene glycol (by-product)	kg/h	737
Sodium sulfate (by-product)	kg/h	3866

Table 6
Reactions involved in the process.

Unit	Stoichiometry
Ball mill	rPET + 2NaOH→$C_2H_6O_2$(EG) + Na_2TPA
Acidification	Na_2TPA + H_2SO_4→TPA + Na_2SO_4
Neutralization	H_2SO_4 + 2NaOH→Na_2SO_4 + 2H_2O
Crystallization	Na_2SO4 + 10 H_2O→Na_2SO4 • 10H_2O

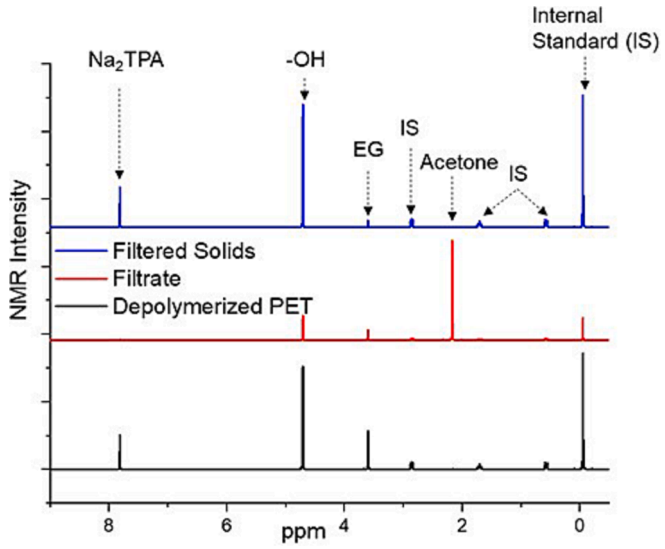

Fig. 4. Solution NMR spectra (in D_2O) of depolymerized PET (black), EG-acetone extraction filtrate (red), and filtered solids (blue). (For interpretation of the references to color in this figure legend, the reader is referred to the web version of this article.)

filtrate after EG extraction with acetone, and filtered solids in D_2O. Equimolar concentrations of terephthalate (~7.8 ppm) in the form of Na_2TPA and EG (~3.5 ppm) were observed in the spectrum of depolymerized PET. The absence of the aromatic proton peak corresponding to Na_2TPA or any unreacted PET in the spectrum of the filtrate indicates the excellent selectivity of EG extraction with acetone. The solution NMR data analysis with DSS as the internal standard showed 98 % EG recovery. A 1:1 ratio by weight of EG to acetone was used for extraction at the laboratory scale. Since EG is miscible in acetone, this ratio was used to provide effective mixing of reactor product solids with acetone (Fig. S1, Supporting Information). EG was recovered with 99 mol% purity with a rotary evaporator (370 mbar, 50 °C) mimicking a single-stage distillation.

To further test the robustness of the process, waste PET textile (with brown dye) from Kolon Industries were tested. Although the presence of dyes in commercial textile samples does not affect the efficiency of extraction of EG with acetone, a significant amount of dye disperses in the acetone phase (Fig. S2a). Activated carbon adsorbents selectively remove the dispersed dyes from the acetone phase (Fig. S2a). These observations are supported by the solution NMR spectrum (Fig. S2b) which shows the presence of characteristic dye peaks (~2.13 ppm) in the acetone phase, and the subsequent disappearance of such peaks after treatment with activated carbon. Complete dissolution of the filtered solids (predominantly Na_2TPA with complete depolymerization) was observed by maintaining the concentration under 10 wt% at room temperature. Residual dye (in commercial samples) dispersed in aqueous Na_2TPA solution was selectively removed with activated carbon (Fig. S3). Additionally, the depolymerization of commercial PET bottles and food containers was also studied (Fig. S4a). Near complete depolymerization of both PET bottles and food containers were obtained withing 20 mins of ball milling (Fig. S4b). Furthermore, solution NMR spectrums of both PET bottles and containers (in TFA-d) show no additives or contaminants (Fig. S4c). Fig. S4d shows the absence of any byproducts (except EG and Na_2TPA) after complete depolymerization of PET bottles and containers. Thus, the proposed process flow and techno-economic analysis are robust towards commercial feed stock such as waste PET textile, PET bottles and food containers.

The precipitation of TPA was performed with the slow acidification of aqueous Na_2TPA solution with slight excess of H_2SO_4 (1.003 times stoichiometric). Solution NMR confirmed 98 % recovery of terephthalic acid from the completely depolymerized PET, similar to earlier observations.[69] Fig. 5a shows the powder XRD pattern of the recovered crystals. The presence of characteristic crystalline peaks confirms the formation of TPA crystals. Fig. 5b compares the NMR spectra of pure and recovered TPA in DMSO-d_6. No significant peaks other than TPA, H_2O, and DMSO can be identified, confirming the excellent purity of rTPA. Fig. 5c and d show magnified plots from Fig. 5b, in which the small peaks present are due to noise/instrumental artifacts.

The recovery of process water was demonstrated with a DuPont XC70 reverse osmosis membrane. The supernatant was neutralized with the addition of stoichiometric NaOH to enhance salt rejection performance. Table 7 shows the salt rejection performance and the flux of process water at 70 bar and room temperature. A feed concentration of 72.73 g/L depicts the initial feed concentration after rTPA precipitation. The 200 g/L of Na_2SO_4 solution represents the brine (end of membrane stage) with ~ 63.6 % water recovered. Significant salt rejections were observed (~95.7 %) at both the starting and brine concentrations. Li et al. also showed similar results with a commercial RO membrane.[70] These data were used to model a membrane unit for water recovery.

3.3. Process simulation and economic analysis

Equipment sizes, and subsequently the overall capital investment, were evaluated based on the mass and energy flows obtained from the process simulation. Information on raw materials flows and energy requirements was utilized to calculate the variable operating costs. The resulting mass flows are summarized in Tables S1 – S5 and Fig. S5. The TCI is projected at $10.6 M, while the bare module cost (Fig. 6) is estimated at $6.2 M. The highest contribution (61.6 %) to the bare module cost is attributed to the product purification steps such as EG distillation, recovery of the rTPA crystals, and Glauber's salt crystallization, and this is mainly due to the capital cost of the distillation column and the salt crystallizer. The initial capital expenses for the downstream separation units are mitigated by the EG and SS stream recovery, which are subsequently sold at their market price. In addition, 21 % of the TCI is estimated for the pretreatment steps that include the necessary machinery for feedstock transportation and storage. The depolymerization section, which includes the ball-mill reactor, accounts for 17.4 % of the total capital expenditure. Table 8 provides a detailed cost breakdown for each unit operation modeled as well as the capital costs (bare module) for each section.

Other than the upfront equipment investment, an annual operating cost of $22 M USD is required for the efficient operation of the facility. As illustrated in Fig. 7, the primary component of the operating expenses is the cost of raw materials. Particularly, the cost of feedstock accounts for 62 % of the raw material costs. In the baseline analysis, it is assumed that the feedstock is derived from the use of clean PET flakes sourced from PET recyclers. The implementation of a pre-treatment section at the production facility, that would shred and clean the PET bales (compressed plastic waste), could significantly reduce the cost of raw materials. More specifically, PET bales are priced at approximately one-sixth the cost of clean flakes, hence, there is potential to make the process even more profitable. As illustrated experimentally, the proposed design is capable of processing commercial waste, demonstrating the practical feasibility of reducing the feedstock cost. Another notable advantage of mechanochemical depolymerization is that it does not require fine particles as feedstock since the sizes of the plastics are

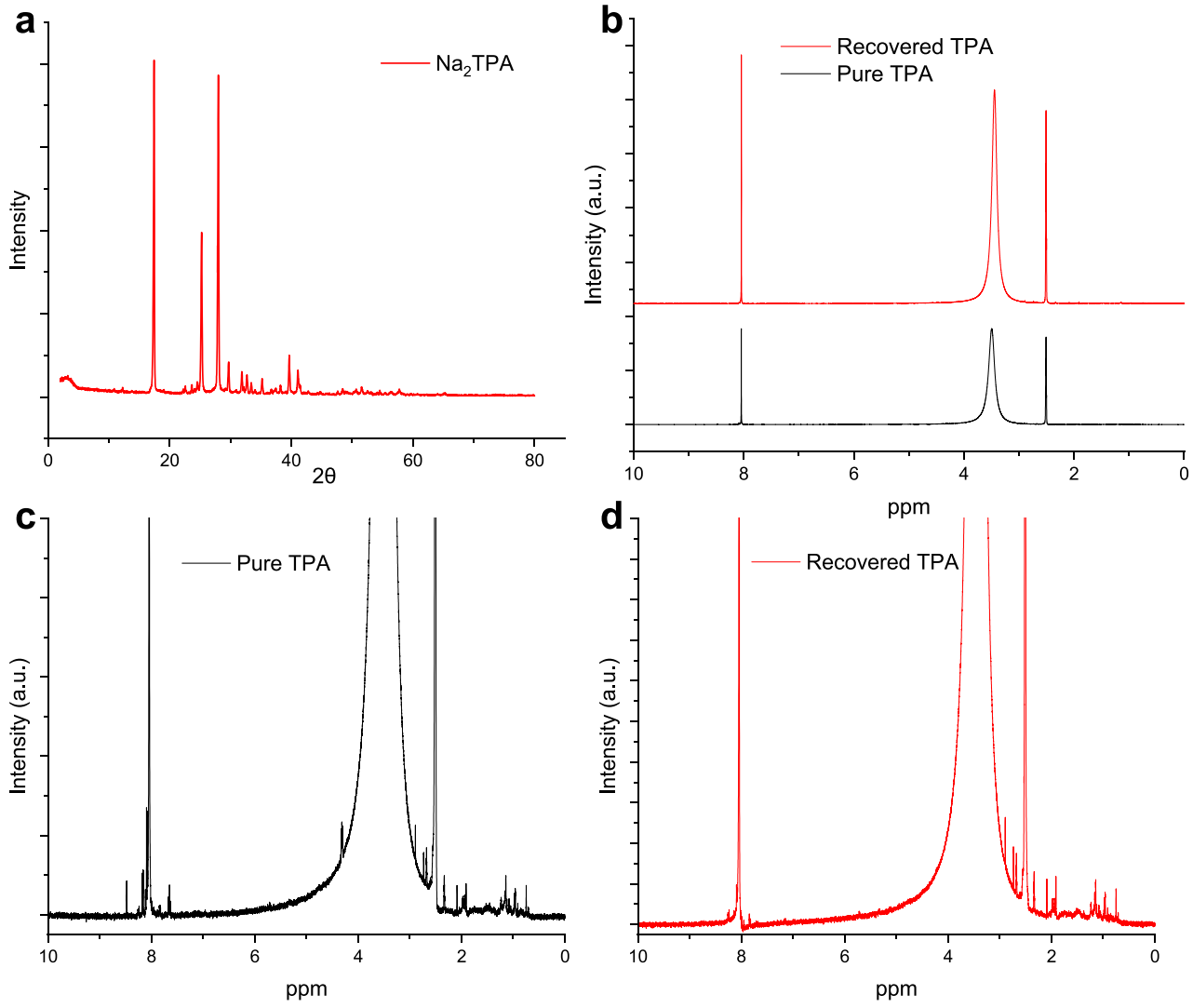

Fig. 5. (a) Powder XRD pattern of recovered TPA, (b) NMR spectra of pure and recovered TPA in DMSO-d_6, (c) and (d) magnified NMR spectra of pure and recovered TPA respectively.

Table 7
Na_2SO_4 salt rejection performance of DuPont XC70 membrane.

Feed Concentration (g/L)	Water Flux (L/m^2/hr)	Salt Rejection (%)
72.73	31.0	96
250	3	92

further reduced during the ball milling process.

The consumption of electricity is a major cost factor in the depolymerization section, primarily required to power the rotation of the milling vessel and the grinding balls. In the crystallization section, the primary cost drivers are the chemicals used for the recovery of rTPA crystals, which are offset by the recovery of sulfate salt in the subsequent process section. Similarly, in the distillation column, the high quantity of steam required for the evaporation of acetone is balanced with the recovery of EG. Additionally, replacement costs for the grinding balls of the ball mill reactor, membrane replacement (every 4 years in the baseline case), activated carbon bed are also accounted for in the economic analysis and are counted as operating expenses. The broad categories of costs and revenue are shown in Table 9.

A discounted cash flow analysis approach was implemented to evaluate the projected break-even point and the rTPA minimum selling price (MSP) produced in this facility, accounting for the revenue from ethylene glycol (EG) and Glauber salt (SS) sales. The net-present-value (NPV) and minimum selling price (MSP) profitability metrics are determined based on the assumptions discussed in a previous section. An MSP of $0.99/kg for rTPA is estimated for the baseline case, indicating that the mechanochemical depolymerization process is competitive with the traditional vTPA (market price is $1.14/kg). In essence, without accounting any profits and considering the assumed market conditions, rTPA is found to be less expensive than fossil derived TPA. Fig. 8 illustrates the cash flow and discounted cash flow of the baseline process, revealing that the process is profitable even for the scenario that ideal feedstock is used.

3.4. Sensitivity analysis

To obtain further insights to the feasibility of the process, a single-point sensitivity analysis is conducted focusing on key-process and economic variables within each section. Through this approach, the potential for additional R&D can be identified and the most significant challenges for commercial success can be emphasized. The engineering parameters and economic assumptions were varied to assess profitability under different scenarios and uncertainty conditions in a plant-scale operation.

Table 10 summarizes the key parameters and their respective upper

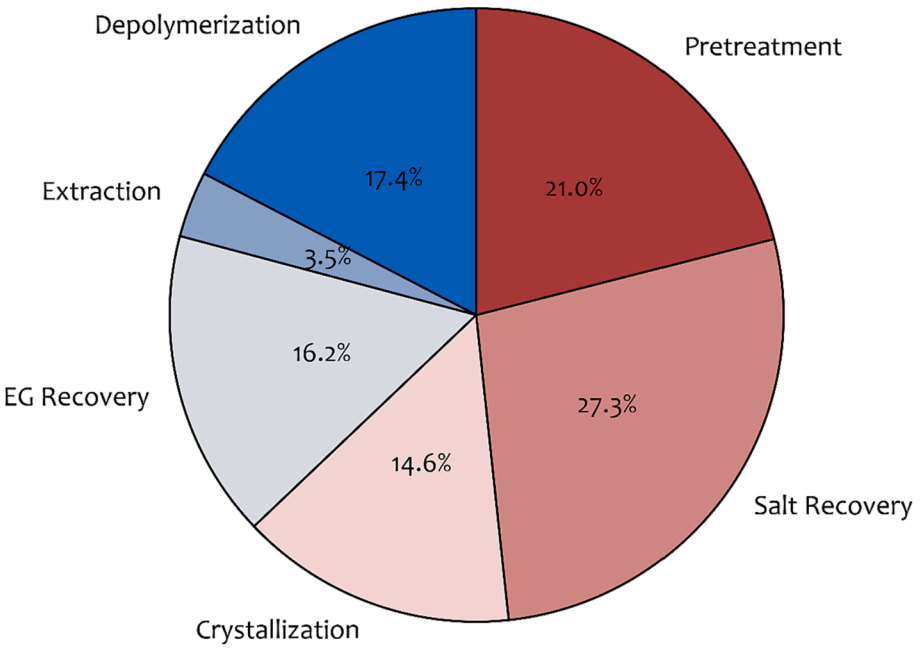

Fig. 6. The bare module cost of $6.2 M split into different process sections.

Table 8
Capital cost (bare module) breakdown for all the processing units for the different regions of the flowsheet. The total capital cost of each of the regions is denoted in bold.

	Capital Cost ($)		Capital Cost ($)
Pretreatment (total)	**$1,309,771**	**Crystallization (total)**	**$909,581**
Conveyor belt	$31,486	Dissolution	$156,121
NaOH tank	$98,243	Filter 2	$127,017
Truck dumper	$283,508	Filter 3	$125,184
Storage dome	$896,534	Acidification	$191,650
Depolymerization (total)	**$1,082,976**	TPA tank	$181,984
Ball Mill	$1,082,976	$H2SO_4$ tank	$127,625
Extraction (total)	**$216,695**	**Salt Recovery (total)**	**$1,700,779**
Extraction Unit	$129,754	Membrane	$352,479
Filter 1	$47,742	Crystallization	$457,762
Activated Carbon 1	$5,288	Neutralization reactor	$220,184
Acetone tank	$33,912	Pump 2	$300,403
EG recovery (total)	**$1,012,525**	SS Filter	$81,632
Distillation column	$872,861	Activated Carbon 2	$25,278
EG tank	$139,664	SS tank	$263,041

and lower bounds, that are expected to significantly impact the projected profitability and are therefore selected for sensitivity analysis. In terms of the reactor consumables, the grinding media lifetime is investigated by varying the degree of wear and tear of the stainless-steel balls. In the case of the reverse osmosis (RO) membrane, its lifespan is selected as a key design parameter. The crystallization temperature is also investigated since it determines the use of an expensive refrigerant (available at −12.2 °C) or cheaper cooling water (available at 4.4 °C) alternative as a cooling medium [57]. Finally, prices of PET bales (feed), raw materials (NaOH), and co-products (EG, SS) are also evaluated to assess their effect on the calculated economic metrics as all these prices are subject to volatility [49]. Their lower and upper bounds were set at +/- 20 % of the baseline price, except for the price of PET waste. A lower bound of $ 0.2/kg and $ 1.0/kg was set for the feedstock to investigate the scenarios that non-ideal feedstocks are used (e.g., PET bales).

In this analysis, we have varied each of the input sensitivity parameters (Table 10) one at a time, which does not account for the impact of parameter correlations on the robustness of the process economics. To justify this approach, a correlation analysis was conducted on historical price data and revealed no significant correlations. A table of historical prices used is provided in the SI (Table S9 and S10). With regards to the process-related sensitivity parameters (i.e., grinding media loss, membrane lifetime, crystallization temperature), no correlation is assumed since these can be independently varied within different unit operations. Therefore, in this study, all the parameters considered are assumed to be independent.

Fig. 9 depicts the impact of the prices of feedstock (PET), co-products (EG,SS), and raw materials (NaOH, H_2SO_4) on the MSP of rTPA. The MSP of the rTPA product is observed to exhibit high sensitivity to the price fluctuations of the waste PET. The NaOH price also has a strong effect on the MSP since it is utilized in large quantities in the depolymerization and salt recovery section. The selling prices of co-products such as EG or SS also appear to impact the price of the final product since they are both sold in high quantities. Finally, the price of H_2SO_4 appears to have minor effect to the resulting MSP, since it is relatively inexpensive compared to all others.

In terms of the process parameters (crystallization temperature, lifespan of the membrane, and the grinding media loss), they all exhibit a minor effect on the MSP compared to the other parameters. This result is attributed to the substantial impact of raw material prices on the overall operating expenses. In fact, the cost of raw materials constitutes 64 % of the total operating cost while the utilities only 2 % of the total operating cost.

Given the relatively high PET waste price volatility over the past decade [49], we performed a detailed sensitivity study covering a range of prices from -$0.1/kg to $1.1/kg to delve deeper into its effect to the process profitability. Negative prices indicate the scenario that incentives are provided to avoid landfilling and promote recycling. As illustrated in Fig. 10, the price of PET feedstock exhibits a linear relationship with the process NPV, with an identified break-even point at a price of $0.68/kg for the PET feedstock given the assumed market prices. Beyond this feedstock price, the NPV becomes negative indicating an unprofitable process. Conversely, below the price of $0.68/kg the processes becomes profitable.

Notably, the modeled feedstock consists of clean PET flakes with very

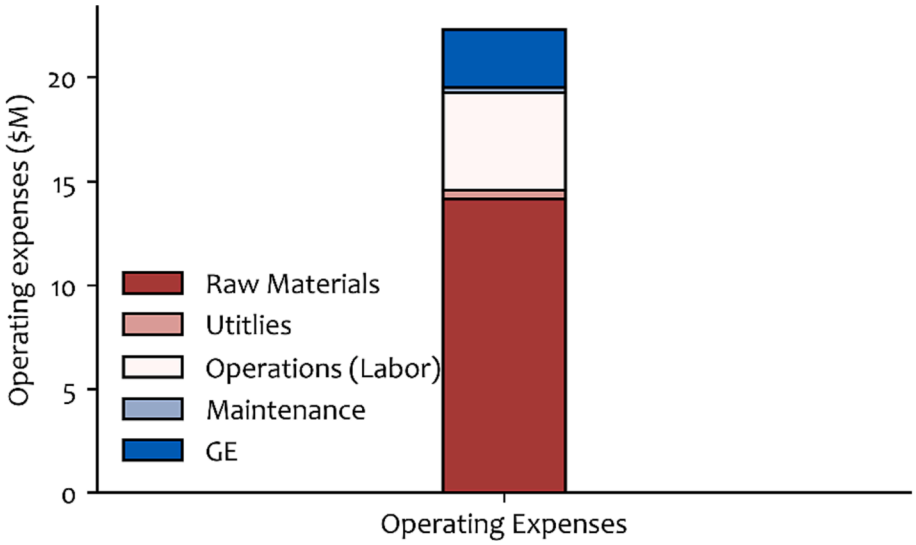

Fig. 7. Operating expenses breakdown.

Table 9
Main costs and sales revenues for baseline mechanochemical plant (2000 kg/h PET).

Category	Cost/Sales ($)
Total capital investment (TCI)	$10,587,425
Cost of Manufacturing (COM)	$20,514,329
Total utility costs	$446,111
Total raw materials	$14,159,020
Total product sales	$27,668,595

small particle sizes and are impurities-, dye- and dirt-free. Based on experimental results, the ball mill reactor can effectively process PET waste of various shapes, sizes, or sources without any impact to the observed conversion or additional pre-milling required since all reactants are milled as processed in the reactor. Therefore, the use of prices of PET bales as feedstock is expected to be representative of an actual industrial application, and the NPV values obtained in Fig. 10 are applicable to such a scenario.

3.5. Technology comparisons

From an economic perspective and under the market assumptions considered in this assessment, the introduction of the mechanochemical PET depolymerization process in the recycling grid is economically profitable. An MSP for rTPA of $0.99/kg was evaluated for mechanochemical milled PET, a price that is directly comparable with the current prices of virgin TPA monomers. In Table 11, we report the MSPs of our proposed design with competing technologies as investigated by Uekert et al. [57]. In both studies, similar assumptions were made with respect to the quality of the feed and final products, the prices of raw materials retrieved from the same source, and similar processing sections were modeled. For the case of methanolysis, we report the price of dimethylterephthalate (DMT) which is the monomer that is used in the production of rPET. It is important to note that these estimates are based on published studies, thus we are not able to estimate uncertainty ranges for these numbers. However, to the best of our knowledge, the resulting MSPs of the fossil- and recycled-based monomers reported in Table 11 are comparable with our study since they account for the same process system boundaries. Uekert et al. [57] also evaluated the MSPs for glycolysis ($0.96/kg) and dissolution ($ 0.87/kg), however, their

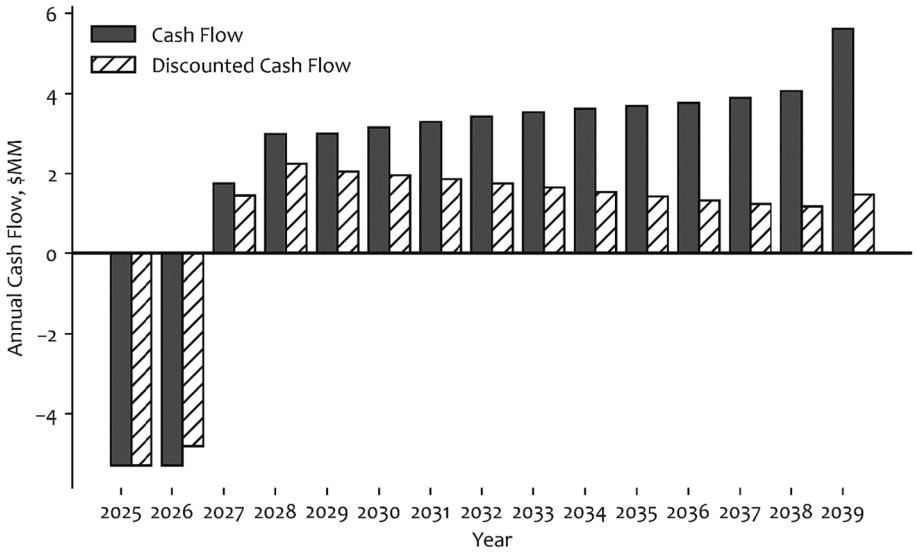

Fig. 8. Annual cash flow in $M for 12 years of operation. The first two years are for commissioning, and hence the sales are zero.

Table 10
Process sensitivity parameters.

Process-specific sensitivity parameters	Base case	Lower bound	Upper bound
Grinding media loss (g/MT media)	50	10	100
RO membrane lifetime (years)	4	1	6
SS Crystallization temperature (°C)	14.4	0.0	14.4
Waste PET price ($/kg)	0.55	0.20	1.00
Co-product price – EG ($/kg)	0.96	−20 %	+20 %
Co-product price – SS ($/kg)	0.15	−20 %	+20 %
Raw material price – NaOH ($/kg)	0.61	−20 %	+20 %
Raw material price – H_2SO_4 ($/kg)	0.10	−20 %	+20 %

analysis included a re-polymerization step at the end of the process sequence to produce rPET, so a direct comparison with the other methods would be unfair. This comparison indicates that the mechanochemical process for PET recycling (as modeled in this study) is expected to be competitive with other closed-loop recycling methods. It is worth noting that both actual selling prices and estimated MSPs highly depend on the market dynamics, supply chain, legislation, and demand for recycled monomers.

The facility size is also expected to drive down the capital and operating costs and increase cost savings by leveraging the benefits of the economies of scale. This applies to all closed-loop recycling technologies that are compared here. As landfilling is increasingly being banned entirely across Europe [71,72], and some US states [73] there will be a growing interest in managing the waste that cannot be landfilled. The smooth operation of any chemical facility is dependent on the steady flow of the feedstock and raw materials hence, the current trend of increased recycling rates is expected to boost the operation of the recycling facility and increase savings.

Mechanochemical recycling is shown here to be a promising technology that could claim a significant share of the current recycling market. This method offers the advantage of high conversion without

Table 11
Estimated MSP for different PET recycling processes.

Technology	MSP ($/kg)	Reference
Virgin	1.14	[49]
Mechanochemical hydrolysis	0.99	This study
Enzymatic hydrolysis	1.93	[49]
Methanolysis (DMT price)	0.96	[57]

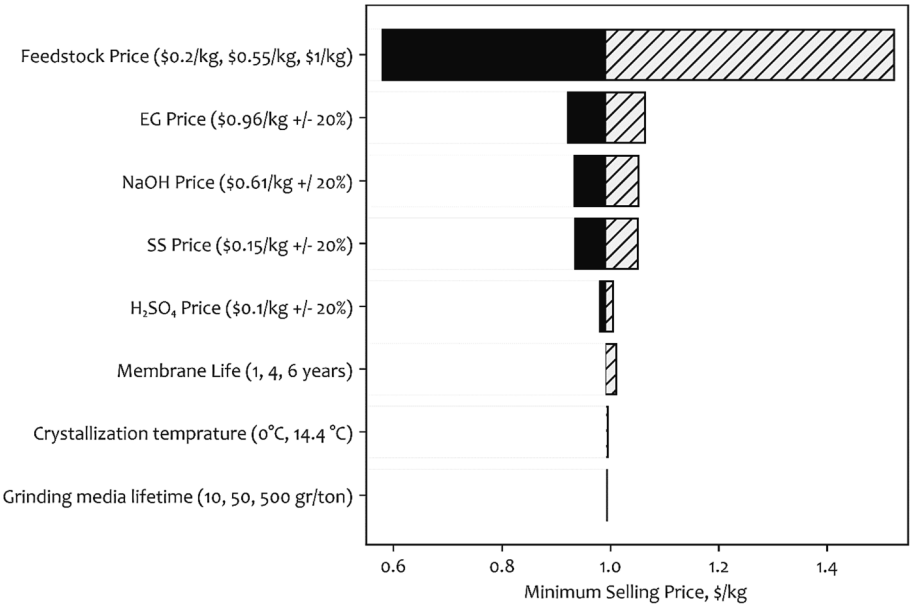

Fig. 9. Change in the TPA MSP as a function of prices of products, co-products, and raw materials; and key process parameters.

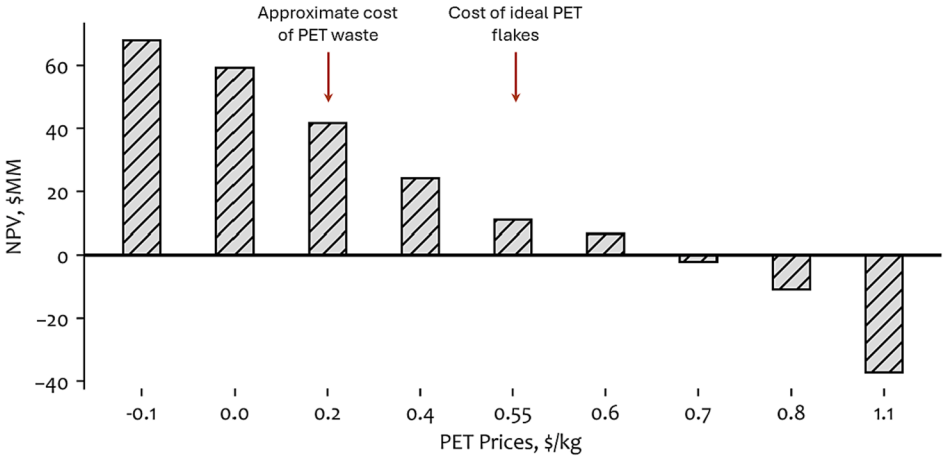

Fig. 10. Net Present Value (NPV) of the mechanochemical process for different waste PET prices.

the need for extreme conditions or pretreatment steps to pre-mill plastic waste to the micron scale. Other plastic feedstocks and depolymerization kinetics should be investigated to enable the holistic investigation of the economic impact of this method in comparison with other recycling technologies. While the operating conditions of the ball mill reactor influence the effectiveness of PET waste depolymerization (e.g., partial or complete depolymerization), efficient separation of products/co-products significantly influences the MSP. In the proposed design any dyes, pigments or adhesives that may be present in the feed are passed through the activated carbon columns and are efficiently removed. Hence, minimizing consumables such as solvents, electricity, steam, and NaOH, many of which are used for the subsequent separation procedures for product recovery, will allow further cost savings. For example, the use of nanofiltration (NF) and RO membranes in series for water recovery could be advantageous, since the NF stage may retain a large fraction of the salt and produce usable water with high flux and lower operating pressure, leaving a much lower volume of NF retentate to be processed by RO to produce additional water. Furthermore, periodic regeneration of the activated carbon bed (before the Na_2SO_4 crystallizer) with recovered process water will enable the recovery of additional rTPA. Finally, the optimization of acetone required for the extraction of EG (at large industrial scale) will significantly reduce distillation costs.

4. Conclusions

In this work, we presented an integrated approach to demonstrate the technical and economic potential of mechanochemical depolymerization of PET. A sequence of unit operations for the downstream purification steps following the ball-mill reactor was designed, experimentally validated at the laboratory scale, and simulated in Aspen Plus. The process flow presented herein enables significant recovery of both TPA (~97 %) and EG (~99 %) as compared to other chemical recycling technologies. Ideal (PET powder) and commercial (bottles, food containers, textiles) samples were examined and used as feedstock to the process. The integrated process is shown to be resilient towards the presence of impurities (such as dyes and pigments) in the feedstock or the use of commercial plastic waste as feedstock (such as textiles, food-grade bottles, and containers). The product quality of rTPA obtained from the mechanochemical recycling process is comparable to petroleum-derived TPA, as opposed to the current industry-standard mechanical recycling.

A techno-economic analysis was also conducted to assess the overall economic viability and critical factors that impact the economics of the process. The findings of the analysis revealed a positive NPV and an evaluated MSP of $0.99/kg for the baseline scenario that utilizes clean PET powder as feedstock. Feedstock prices and purification steps account for a large portion of the operational and capital expenditures, respectively. The downstream purification steps dictate the final selling price of rTPA, as their integration with the reactor enables the efficient recovery and sale of co-products in large quantities. Results from sensitivity analysis show that the process is highly sensitive to the prices of feedstock and raw materials. In the investigated scenarios that PET waste bales are purchased and used as inputs instead of ideal clean PET powder, the process becomes even more profitable. Furthermore, the process designed in this manuscript is competitive with conventional fossil-based sources and alternative recycling pathways as the calculated MSP is at par with the vTPA and rTPA prices. While the framework outlined in this work primarily targets PET waste, a similar mechanochemical or mechanocatalytic approach can be applied to other waste polymer feedstocks.

Finally, it should be noted that the models utilized in this study are based on conversions observed at the laboratory scale. To account for deviations and additional degrees of freedom of the process sequence at larger scale, future work will include the development of detailed models and further experimentation. Moreover, the combination of process, supply chain, and life cycle assessment (LCA) will enable a full evaluation of the environmental factors and social-economic impacts of this technology, such as GHG emissions. This will enable a holistic comparison of mechanochemical depolymerization relative to other recycling technologies and allow the identification of an optimal supply chain of recycling processes. The outcome of the analysis presented herein provides yield and economics metrics for a complete mechanochemical process for recycling of PET waste. Such studies are necessary to assess the potential feasibility of new technologies, and for developing policies that incentivize industries to pursue pathways that promote chemical recycling, in anticipation of the transition to a complete circular economic model for plastics.

CRediT authorship contribution statement

Elisavet Anglou: Conceptualization, Data curation, Formal analysis, Methodology, Investigation, Visualization, Validation, Writing – original draft, Writing – review & editing. **Arvind Ganesan:** Conceptualization, Data curation, Formal analysis, Methodology, Investigation, Visualization, Validation, Writing – original draft, Writing – review & editing. **Yuchen Chang:** Data curation, Writing – review & editing. **Kinga M. Gołąbek:** Data curation, Writing – review & editing. **Qiang Fu:** Data curation. **William Bradley:** Methodology, Writing – review & editing. **Christopher W. Jones:** Conceptualization, Methodology, Supervision, Funding acquisition, Writing – review & editing. **Carsten Sievers:** Conceptualization, Methodology, Supervision, Funding acquisition, Project administration, Writing – review & editing. **Sankar Nair:** Conceptualization, Methodology, Supervision, Funding acquisition, Writing – review & editing. **Fani Boukouvala:** Conceptualization, Methodology, Supervision, Funding acquisition, Writing – review & editing.

Declaration of competing interest

The authors declare the following financial interests/personal relationships which may be considered as potential competing interests: Carsten Sievers, Sankar Nair, Christopher Jones, and Fani Boukouvala have a provisional patent application filled in the U.S. Patent and Trademark Office as U.S. Patent Application serial No.: 17/801,027 to Georgia Tech Research Corporation.

Data availability

Data will be made available on request.

Acknowledgements

The work was financially supported by Kolon Industries, Inc. through the Kolon Center for Lifestyle Innovation at Georgia Institute of Technology, and the U.S. National Science Foundation – Emerging Frontiers in Research and Innovation program under grant 2028998.

Appendix A. Supplementary data

Supplementary data to this article can be found online at https://doi.org/10.1016/j.cej.2023.148278.

References

[1] R. Geyer, J.R. Jambeck, K.L. Law, Production, use, and fate of all plastics ever made, Sci Adv. 3 (2017) 25–29, https://doi.org/10.1126/sciadv.1700782.
[2] I. Vollmer, M.J.F. Jenks, M.C.P. Roelands, R.J. White, T. van Harmelen, P. de Wild, G.P. van der Laan, F. Meirer, J.T.F. Keurentjes, B.M. Weckhuysen, Beyond Mechanical Recycling: Giving New Life to Plastic Waste, Angew Chem Int Ed Engl. 59 (2020) 15402–15423, https://doi.org/10.1002/anie.201915651.
[3] L.E. Revell, P. Kuma, E.C. Le Ru, W.R.C. Somerville, S. Gaw, Direct radiative effects of airborne microplastics, Nature. 598 (2021) 462–467, https://doi.org/10.1038/s41586-021-03864-x.

[4] L.C. Jenner, J.M. Rotchell, R.T. Bennett, M. Cowen, V. Tentzeris, L.R. Sadofsky, Detection of microplastics in human lung tissue using μFTIR spectroscopy, Science of the Total Environment. 831 (2022), https://doi.org/10.1016/j.scitotenv.2022.154907.

[5] P.S. Ross, S. Chastain, E. Vassilenko, A. Etemadifar, S. Zimmermann, S.A. Quesnel, J. Eert, E. Solomon, S. Patankar, A.M. Posacka, B. Williams, Pervasive distribution of polyester fibres in the Arctic Ocean is driven by Atlantic inputs, Nat Commun. 12 (2021), https://doi.org/10.1038/s41467-020-20347-1.

[6] T. Tiso, T. Narancic, R. Wei, E. Pollet, N. Beagan, K. Schröder, A. Honak, M. Jiang, S.T. Kenny, N. Wierckx, R. Perrin, L. Avérous, W. Zimmermann, K. O'Connor, L. M. Blank, Towards bio-upcycling of polyethylene terephthalate, Metab Eng. 66 (2021) 167–178, https://doi.org/10.1016/J.YMBEN.2021.03.011.

[7] H. Li, H.A. Aguirre-Villegas, R.D. Allen, X. Bai, C.H. Benson, G.T. Beckham, S. L. Bradshaw, J.L. Brown, R.C. Brown, V.S. Cecon, J.B. Curley, G.W. Curtzwiler, S. Dong, S. Gaddameedi, J.E. García, I. Hermans, M.S. Kim, J. Ma, L.O. Mark, M. Mavrikakis, O.O. Olafasakin, T.A. Osswald, K.G. Papanikolaou, H. Radhakrishnan, M.A. Sanchez Castillo, K.L. Sánchez-Rivera, K.N. Tumu, R. C. Van Lehn, K.L. Vorst, M.M. Wright, J. Wu, V.M. Zavala, P. Zhou, G.W. Huber, Expanding plastics recycling technologies: chemical aspects, technology status and challenges, Green Chemistry. 24 (2022), https://doi.org/10.1039/d2gc02588d.

[8] Z. Jagiello, M. Corsini, Ł. Dylewski, J.D. Ibáñez-Álamo, M. Szulkin, The Extended Avian Urban Phenotype Impact of Anthropogenic Debris Pollution on Nest Design and Fitness, SSRN Electronic Journal. (2022), https://doi.org/10.2139/SSRN.4020176.

[9] K.R. Nicastro, L. Seuront, C.D. McQuaid, G.I. Zardi, Symbiont-induced intraspecific phenotypic variation enhances plastic trapping and ingestion in biogenic habitats, Science of the Total Environment. 826 (2022) 153922, https://doi.org/10.1016/J.SCITOTENV.2022.153922.

[10] J.M. Sipe, N. Bossa, W. Berger, N. von Windheim, K. Gall, M.R. Wiesner, From bottle to microplastics: Can we estimate how our plastic products are breaking down? Science of the Total Environment. 814 (2022) 152460 https://doi.org/10.1016/J.SCITOTENV.2021.152460.

[11] A.N. Walsh, C.M. Reddy, S.F. Niles, A.M. McKenna, C.M. Hansel, C.P. Ward, Plastic Formulation is an Emerging Control of Its Photochemical Fate in the Ocean, Environ Sci Technol. 55 (2021) 12383–12392, https://doi.org/10.1021/ACS.EST.1C02272/SUPPL_FILE/ES1C02272_SI_001.PDF.

[12] Researchers Engineer Microorganisms To Tackle PET Plastic Pollution | News | NREL, (n.d.). https://www.nrel.gov/news/program/2021/researchers-engineer-microorganisms-to-tackle-pet-plastic-pollution.html (accessed March 10, 2022).

[13] J.M. Garcia, M.L. Robertson, The future of plastics recycling, Science 358 (2017) (1979) 870–872.

[14] T. Thiounn, R.C. Smith, Advances and approaches for chemical recycling of plastic waste, Journal of Polymer Science. 58 (2020) 1347–1364, https://doi.org/10.1002/pol.20190261.

[15] S.M. Al-Salem, P. Lettieri, J. Baeyens, Recycling and recovery routes of plastic solid waste (PSW): A review, Waste Management. 29 (2009) 2625–2643, https://doi.org/10.1016/j.wasman.2009.06.004.

[16] J. Ma, P.A. Tominac, H.A. Aguirre-Villegas, O.O. Olafasakin, M.M. Wright, C. H. Benson, G.W. Huber, V.M. Zavala, Economic evaluation of infrastructures for thermochemical upcycling of post-consumer plastic waste, Green Chemistry. 25 (2023) 1032–1044.

[17] K. Ragaert, L. Delva, K. Van Geem, Mechanical and chemical recycling of solid plastic waste, Waste Management. 69 (2017) 24–58, https://doi.org/10.1016/j.wasman.2017.07.044.

[18] E. Barnard, J.J. Rubio Arias, W. Thielemans, Chemolytic depolymerisation of PET: a review, Green Chemistry. 23 (2021) 3765–3789, https://doi.org/10.1039/d1gc00887k.

[19] A.W. Tricker, A.A. Osibo, Y. Chang, J.X. Kang, A. Ganesan, E. Anglou, F. Boukouvala, S. Nair, C.W. Jones, C. Sievers, Stages and Kinetics of Mechanochemical Depolymerization of Poly (ethylene terephthalate) with Sodium Hydroxide, ACS Sustain Chem Eng. (2022).

[20] C. Sempels, J. Hoffmann, Circular Economy, Sustainable Innovation, Strategy. (2013) 6–9, https://doi.org/10.1057/9781137352613.0008.

[21] I. Nishimura, Strategy for Plastics in a Circular Economy, Seikei-Kakou. 30 (2018) 577–580, https://doi.org/10.4325/seikeikakou.30.577.

[22] R. Meys, F. Frick, S. Westhues, A. Sternberg, J. Klankermayer, A. Bardow, Towards a circular economy for plastic packaging wastes – the environmental potential of chemical recycling, Resour Conserv Recycl. 162 (2020), https://doi.org/10.1016/j.resconrec.2020.105010.

[23] T. Helmer Pedersen, F. Conti, Improving the circular economy via hydrothermal processing of high-density waste plastics, Waste Management. 68 (2017) 24–31, https://doi.org/10.1016/j.wasman.2017.06.002.

[24] S.D. Mancini, M. Zanin, Post Consumer Pet Depolymerization by Acid Hydrolysis, Http://Dx.Doi.Org/10.1080/03602550601152945. 46 (2007) 135–144, https://doi.org/10.1080/03602550601152945.

[25] S. Mishra, A.S. Goje, V.S. Zope, Chemical Recycling, Kinetics, and Thermodynamics of Poly (Ethylene Terephthalate) (PET) Waste Powder by Nitric Acid Hydrolysis, Http://Dx.Doi.Org/10.1081/PRE-120018586. 11 (2017) 79–99. https://doi.org/10.1081/PRE-120018586.

[26] T. Yoshioka, N. Okayama, A. Okuwaki, Kinetics of Hydrolysis of PET Powder in Nitric Acid by a Modified Shrinking-Core Model, Ind Eng Chem Res. 37 (1998) 336–340, https://doi.org/10.1021/IE970459A.

[27] A. Palme, A. Peterson, H. de la Motte, H. Theliander, H. Brelid, Development of an efficient route for combined recycling of PET and cotton from mixed fabrics, Textiles and Clothing Sustainability. 3 (2017), https://doi.org/10.1186/s40689-017-0026-9.

[28] M. Barth, R. Wei, T. Oeser, J. Then, J. Schmidt, F. Wohlgemuth, W. Zimmermann, Enzymatic hydrolysis of polyethylene terephthalate films in an ultrafiltration membrane reactor, J Memb Sci. 494 (2015) 182–187, https://doi.org/10.1016/j.memsci.2015.07.030.

[29] J.A. Schwartz, P.E.A. Acquah, United States Patent (19), 54 (1995).

[30] R. López-Fonseca, M.P. González-Marcos, J.R. González-Velasco, J.I. Gutiérrez-Ortiz, Chemical recycling of PET by alkaline hydrolysis in the presence of quaternary phosphonium and ammonium salts as phase transfer catalysts, WIT Transactions on Ecology and the Environment. 109 (2008) 511–520, https://doi.org/10.2495/WM080521.

[31] J.V. Valh, B. Vončina, A. Lobnik, L.F. Zemljič, L. Škodič, S. Vajnhandl, Conversion of polyethylene terephthalate to high-quality terephthalic acid by hydrothermal hydrolysis: the study of process parameters, Textile Research Journal. 90 (2020) 1446–1461, https://doi.org/10.1177/0040517519893714.

[32] S.D. Mancini, M. Zanin, Optimization of Neutral Hydrolysis Reaction of Post-Consumer PET for Chemical Recycling 20 (2004).

[33] F. Chen, G. Wang, W. Li, F. Yang, Glycolysis of poly(ethylene terephthalate) over Mg-Al mixed oxides catalysts derived from hydrotalcites, Ind Eng Chem Res. 52 (2013) 565–571, https://doi.org/10.1021/ie302091j.

[34] Q. Wang, Y. Geng, X. Lu, S. Zhang, First-row transition metal-containing ionic liquids as highly active catalysts for the glycolysis of poly(ethylene terephthalate) (PET), ACS Sustain Chem Eng. 3 (2015) 340–348, https://doi.org/10.1021/sc5007522.

[35] Y. Liu, X. Yao, H. Yao, Q. Zhou, J. Xin, X. Lu, S. Zhang, Degradation of poly (ethylene terephthalate) catalyzed by metal-free choline-based ionic liquids, Green Chemistry. 22 (2020) 3122–3131, https://doi.org/10.1039/d0gc00327a.

[36] B. Allen, G. Breyta, J. Garcia, G. Jones, J. Hedrick, Polyester Digestion : VOLCAT Summit on Realizing the IBM Materials Innovation, Polymer Materials (2018).

[37] Y. Asakuma, Y. Yamamura, K. Nakagawa, K. Maeda, K. Fukui, Mechanism of Depolymerization Reaction of Polyethylene Terephthalate: Experimental and Theoretical Studies, J Polym Environ. 19 (2011) 209–216, https://doi.org/10.1007/s10924-010-0263-3.

[38] M. Han, Depolymerization of PET Bottle via Methanolysis and Hydrolysis, Recycling of Polyethylene Terephthalate Bottles. (2019) 85–108, https://doi.org/10.1016/B978-0-12-811361-5.00005-5.

[39] V. Štrukil, Highly Efficient Solid-State Hydrolysis of Waste Polyethylene Terephthalate by Mechanochemical Milling and Vapor-Assisted Aging, ChemSusChem. (2020), https://doi.org/10.1002/cssc.202002124.

[40] A.W. Tricker, K.L. Hebisch, M. Buchmann, Y.-H. Liu, M. Rose, E. Stavitski, A. J. Medford, M.C. Hatzell, C. Sievers, Mechanocatalytic Ammonia Synthesis over TiN in Transient Microenvironments, ACS Energy Lett. 5 (2020) 3362–3367, https://doi.org/10.1021/acsenergylett.0c01895.

[41] J. Lu, S. Borjigin, S. Kumagai, T. Kameda, Y. Saito, T. Yoshioka, Practical dechlorination of polyvinyl chloride wastes in NaOH/ethylene glycol using an up-scale ball mill reactor and validation by discrete element method simulations, Waste Management. 99 (2019) 31–41.

[42] E. Jung, D. Yim, H. Kim, G.I. Peterson, T. Choi, Depolymerization of poly (α-methyl styrene) with ball-mill grinding, Journal of Polymer Science. 61 (2023) 553–560.

[43] M. Baláž, Z. Bujňáková, M. Achimovičová, M. Tešinský, P. Baláž, Simultaneous valorization of polyvinyl chloride and eggshell wastes by a semi-industrial mechanochemical approach, Environ Res. 170 (2019) 332–336.

[44] V.P. Balema, I.Z. Hlova, S.L. Carnahan, M. Seyedi, O. Dolotko, A.J. Rossini, I. Luzinov, Depolymerization of polystyrene under ambient conditions, New Journal of Chemistry. 45 (2021) 2935–2938.

[45] J. Zhao, Y. Shu, Q. Niu, P. Zhang, Processing Plastic Wastes into Value-Added Carbon Adsorbents by Sulfur-Based Solvothermal Synthesis, ACS Sustain Chem Eng. 11 (2023) 11207–11218, https://doi.org/10.1021/acssuschemeng.3c02049.

[46] J. Zhao, Q. Niu, J. Zhang, P. Zhang, Core-shell construction of metal@carbon by mechanochemically recycling plastic wastes: towards an efficient oxygen evolution reaction, Green Chemistry. 25 (2023) 8047–8056, https://doi.org/10.1039/d3gc02695g.

[47] S. Aydonat, A.H. Hergesell, C.L. Seitzinger, R. Lennarz, Y. Chang, C. Sievers, J. Meisner, I. Vollmer, R. Göstl, Leveraging mechanochemistry for sustainable polymer degradation, Polymer Journal (accepted) (2023).

[48] A. Aguado, L. Martínez, L. Becerra, M. Arieta-araunabeña, S. Arnaiz, A. Asueta, I. Robertson, Chemical depolymerisation of PET complex waste: Hydrolysis vs. glycolysis, J Mater Cycles Waste Manag. 16 (2014) 201–210, https://doi.org/10.1007/s10163-013-0177-y.

[49] A. Singh, N.A. Rorrer, S.R. Nicholson, E. Erickson, J.S. DesVeaux, A.F.T. Avelino, P. Lamers, A. Bhatt, Y. Zhang, G. Avery, Techno-economic, life-cycle, and socioeconomic impact analysis of enzymatic recycling of poly (ethylene terephthalate), Joule. 5 (2021) 2479–2503.

[50] Aspen Plus, Aspen Technology V12.1 User guide, Inc., Cambridge, MA. (n.d.).

[51] P.S.E. Ltd., gProms advanced user guide, (2004).

[52] F. Boukouvala, R. Ramachandran, A. Vanarase, F.J. Muzzio, M.G. Ierapetritou, Computer Aided Design and Analysis of Continuous Pharmaceutical Manufacturing Processes, in: E.N. Pistikopoulos, M.C. Georgiadis, A.C. Kokossis (Eds.), Computer Aided Chemical Engineering, Elsevier, 2011: pp. 216–220. https://doi.org/https://doi.org/10.1016/B978-0-444-53711-9.50044-4.

[53] Z. Wang, C. Ma, A. Shen, A. Berchenko, S.A. Sinquefield, S. Nair, Kraft black liquor concentration with graphene oxide membranes: Process simulations and technoeconomic analysis, J Adv Manuf Process. 3 (2021) e10104–e.

[54] G. Stephanopoulos, G.V. Reklaitis, Process systems engineering: From Solvay to modern bio- and nanotechnology. A history of development, successes and prospects for the future, Chem Eng Sci. 66 (2011) 4272–4306, https://doi.org/10.1016/j.ces.2011.05.049.

[55] Y. Luo, E. Selvam, D.G. Vlachos, M. Ierapetritou, Economic and Environmental Benefits of Modular Microwave-Assisted Polyethylene Terephthalate Depolymerization, ACS Sustain Chem Eng. 11 (2023) 4209–4218, https://doi.org/10.1021/acssuschemeng.2c07203.
[56] B. Hernández, P. Kots, E. Selvam, D.G. Vlachos, M.G. Ierapetritou, Techno-Economic and Life Cycle Analyses of Thermochemical Upcycling Technologies of Low-Density Polyethylene Waste, ACS Sustain Chem Eng. 11 (2023) 7170–7181, https://doi.org/10.1021/acssuschemeng.3c00636.
[57] T. Uekert, A. Singh, J.S. DesVeaux, T. Ghosh, A. Bhatt, G. Yadav, S. Afzal, J. Walzberg, K.M. Knauer, S.R. Nicholson, G.T. Beckham, A.C. Carpenter, Technical, Economic, and Environmental Comparison of Closed-Loop Recycling Technologies for Common Plastics, ACS Sustain Chem Eng. 11 (2023) 965–978, https://doi.org/10.1021/acssuschemeng.2c05497.
[58] T. Uekert, A. Singh, J.S. DesVeaux, T. Ghosh, A. Bhatt, G. Yadav, S. Afzal, J. Walzberg, K.M. Knauer, S.R. Nicholson, Technical, Economic, and Environmental Comparison of Closed-Loop Recycling Technologies for Common Plastics, ACS Sustain Chem Eng. (2023).
[59] Altair EDEM 2021.1 Simulation Software, (n.d.).
[60] X. Bian, G. Wang, H. Wang, S. Wang, W. Lv, Effect of lifters and mill speed on particle behaviour, torque, and power consumption of a tumbling ball mill: Experimental study and DEM simulation, Miner Eng. 105 (2017) 22–35, https://doi.org/10.1016/j.mineng.2016.12.014.
[61] W.D. Seider, J.D. Seader, D.R. Lewin, S. Widagdo, Product and process design principles: synthesis, Analysis and Evaluation. 4 (2004).
[62] E. Anglou, Y. Chang, A. Ganesan, S. Nair, C. Sievers, F. Boukouvala, Discrete Element Simulation and Economics of Mechanochemical Grinding of Plastic Waste at an Industrial Scale, in, Computer Aided Chemical Engineering, Elsevier (2023) 2405–2410.
[63] D.A. Longhurst, Economics and methodology of ball mill media maintenance, in: 2010 IEEE-IAS/PCA 52nd Cement Industry Technical Conference, IEEE, 2010: pp. 1–20.
[64] C. Swart, J.M. Gaylard, M.M. Bwalya, A Technical and Economic Comparison of Ball Mill Limestone Comminution with a Vertical Roller Mill, Mineral Processing and Extractive Metallurgy Review. 43 (2022) 275–282.
[65] Postconsumer PET Recycling Activity in 2018, (n.d.). https://doi.org/https://napcor.com/wp-content/uploads/2021/07/Postconsumer-PET-Recycling-Activity-in-2018.pdf.
[66] ICIS Database, (n.d.). https://www.icis.com/subscriber/icb/2017/03/01/10083538/us-acetone-faces-prolonged-tightness/#_=_(accessed December 5, 2023).
[67] L. Dessbesell, Z. Yuan, S. Hamilton, M. Leitch, R. Pulkki, C. Xu, Bio-based polymers production in a kraft lignin biorefinery: techno-economic assessment, Biofuels, Bioproducts and Biorefining. 12 (2018) 239–250.
[68] V. Pham, M. Holtzapple, M.M. El-Halwagi, Technoeconomic analysis of a lignocellulose-to-hydrocarbons process using a carboxylate platform, Integrated Biorefineries: Design, Analysis, and Optimization. (2013) 157–192.
[69] G.E. Brown, R.C. O, Method for recovering terephthalic acid and ethylene glycol from polyester materials, (1974).
[70] W. Li, B. Van der Bruggen, P. Luis, Integration of reverse osmosis and membrane crystallization for sodium sulphate recovery, Chemical Engineering and Processing: Process Intensification. 85 (2014) 57–68, https://doi.org/10.1016/J.CEP.2014.08.003.
[71] P. Europe, Plastics—The Facts 2016, An Analysis of European Plastics Production, Demand and Waste Data. (2016) 1–38.
[72] I.M. Steensgaard, K. Syberg, S. Rist, N.B. Hartmann, A. Boldrin, S.F. Hansen, From macro-to microplastics-Analysis of EU regulation along the life cycle of plastic bags, Environmental Pollution. 224 (2017) 289–299.
[73] Vermont Government, Department of Environmental Conservation, (n.d.). https://dec.vermont.gov/waste-management/solid/materials-mgmt/what-happens-my-stuff (accessed June 14, 2023).